

Short-range local order of the Co/Si(111) interface studied by the extended Auger fine-structure technique

J. Y. Veuillen and A. Bensaoula

Laboratoire d'Etudes des Propriétés Electroniques des Solides, Centre National de la Recherche Scientifique, Boîte Postale 166, 38042 Grenoble CEDEX, France

M. De Crescenzi* and J. Derrien

Centre de Recherche sur les Mécanismes de la Croissance Cristalline, Centre National de la Recherche Scientifique, Case 913, 13288 Marseille CEDEX 09, France

(Received 12 September 1988)

Extended Auger fine-structure (EXFAS) spectra have been successfully recorded on ultrathin films of cobalt deposited on silicon (111) surface. Thanks to a detailed comparison of the static disorder of the interface, the short-range order characteristics of EXFAS and its surface-structural sensitivity have been clearly demonstrated.

The study of electrons reemitted from solid surfaces has greatly contributed to a detailed understanding of phenomena occurring at the outermost atomic layers of the investigated samples. So far Auger-electron spectroscopy has been widely used to get information on the chemical composition of a solid surface.¹ Very recently we have demonstrated that fine structures observed in the electron-energy distribution above CVV Auger lines of several transition metals can be used to determine the local order of these samples.² We have attributed the physical origins of these extended fine Auger structures (hereafter called EXFAS) to the same interference mechanisms which produce extended x-ray-absorption fine structure (EXAFS) usually observed in the x-ray photo-absorption spectra.³ Our explanation of fine structures in Auger spectra is, in fact, a natural extension of the autoionization emission associated with direct recombination of a core electron initially excited into the continuum states.⁴ These continuum states contain EXAFS-like features extending on several hundreds of electron volts.⁵ The energy relaxed during the core-electron recombination with its own hole is used to eject into vacuum a valence electron. Measuring the kinetic-energy distribution of these emitted valence electrons (i.e., EXFAS) one can probe the final states of the excited core electrons and therefore reproduce the EXAFS-like features which are connected to the local order of the sample.⁵

Experimental observation of EXFAS signal is very difficult because of its low yield, except in the case of a very narrow, high-density d valence band. This is the reason why up to date EXFAS results are only reported on $3d$ or $4d$ transition-metal surfaces.^{2,7,8} The fine structures observed in Auger spectra had been observed in the past by several authors.^{7,8} Thanks to empirical characteristics of their experimental results these authors^{7,8} suggested a diffraction process [low-energy electron diffraction (LEED)] based on long-range order as a possible cause of the EXFAS features, rather than a scattering

process based on a short-range order (EXAFS-like mechanism).

We report here on an EXFAS study of ultrathin layers of cobalt deposited on silicon (111). The results obtained with this system allow us to remove this controversy and to assess definitively the short-range-order characteristics of the EXFAS features. In particular, we will show that EXFAS cannot be observed on a clean well-ordered (7×7) silicon (111) surface, which is contradictory to the long-range-order suggestion, while with small Co amounts deposited on this Si surface, EXFAS features immediately appear although the Co/Si(111) interfaces are more or less disordered as testified by the Si LEED diagram disappearance with increasing Co coverage, favoring rather the short-range-order suggestion. Moreover, from the analysis of EXFAS features we were able to follow the Co/Si(111) interface formation for the first time with this technique, in complete agreement with previous investigations using other surface techniques. Therefore, our experimental results presented here clearly demonstrate also the wide applicability and usefulness of the EXFAS technique as a structural probe for surfaces and interfaces of d elements and related compounds.

Prior to the EXFAS results presentation let us discuss the Co/Si state of the art. This system has been extensively investigated in the past because of both fundamental and technological interests. It has been demonstrated that quasiperfect epitaxial CoSi_2 layers may be formed by simply annealing to higher temperatures ($\geq 600^\circ\text{C}$) Co thin films previously deposited at room temperature (RT) on Si substrates.⁹⁻¹⁴ These $\text{CoSi}_2/\text{Si}(111)$ heterostructures display a very sharp interface on the monolayer scale.¹⁵ Further, new transistor devices have been achieved based on the reepitaxy of Si on CoSi_2 leading to Si/ CoSi_2 /Si heterostructures.¹⁵⁻¹⁷ The understanding of the mechanisms of silicide formation on top of a Si substrate is of paramount importance and of particular in-

terest are the initial stages of the interface development during Co deposition at room temperature. So far all measurements performed on the (RT) Co/Si(111) interface prepared under ultrahigh-vacuum (UHV) conditions plead for an initial CoSi_2 -like phase within a very low Co-coverage range $\Theta \lesssim 4 \text{ \AA}$. With increasing coverage ($\Theta \lesssim 10 \text{ \AA}$) other Co-richer silicide phases may be observed (CoSi and Co_2Si , respectively) and, finally, an almost pure Co layer spreads on this silicide transition zone. This interface development has been modeled thanks to a tremendous number of surface techniques such as low-energy electron diffraction (LEED), Auger-electron, and photoemission spectroscopy,^{9,13,14} electron-energy-loss fine structure,¹⁸ electrical measurements,¹⁹ and cross-sectional high-resolution electron microscopy.²⁰

All experiments reported here was performed in an UHV chamber (base pressure $\sim 10^{-10}$ Torr) equipped with LEED and various electron-spectroscopy facilities. The Si substrates were cleaned with conventional ion-etching and -annealing cycles to obtain the well-known (7×7) Si(111) reconstructed surfaces. Co atoms were then deposited with a miniature homemade electron-gun evaporator especially designed to work under UHV conditions. The Co evaporation rate (a few \AA per minute)

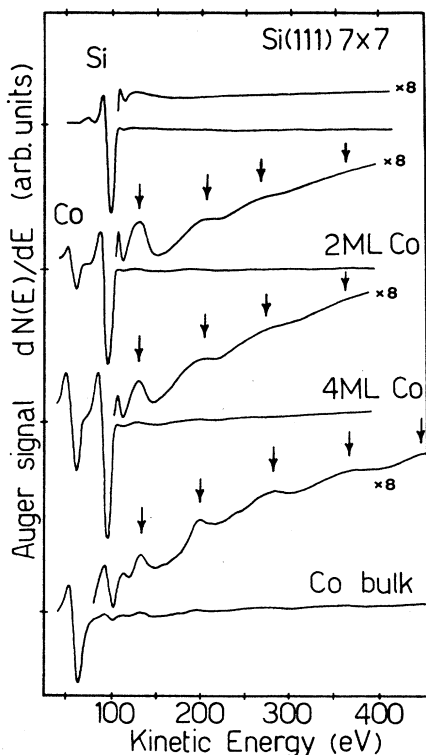


FIG. 1. Auger spectra on Si(111) at various stages of Co deposition. From the top to bottom curves the Co coverages are 0, 2, 4, and ~ 120 monolayers, respectively. Magnification ($\times 8$) of the background allows us to observe reproducible fine structures (EXFAS) marked by arrows. Spectra are not normalized in intensity.

was calibrated by an *in situ* quartz microbalance. Sequential deposits of Co were performed on Si and characterized with various surface techniques in order to recover all previously mentioned results. They will not be reproduced here and only EXFAS will be discussed.

Figure 1 shows the Auger spectra recorded in the first-derivative mode dN/dE on Si(111) at various stages of Co deposition, with identical experimental conditions [incident-electron energy $\sim 3 \text{ keV}$, electron beam $\sim 1 \mu\text{A}$, modulation voltage $\sim 8 \text{ eV}$ (peak to peak)]. Magnifications ($\times 8$) of the background signal above the

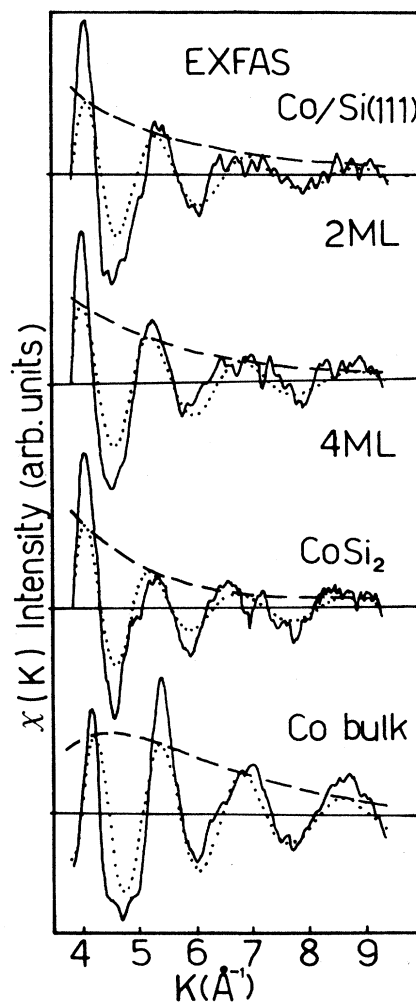


FIG. 2. Solid line: $\chi(k)$ of the EXFAS structures from Fig. 1 obtained after a background subtraction and wave-vector k -space transform using the E_0 threshold energy at the $\text{Co } M_{2,3}VV$ line for evaluating the electron wave vector k , with $k = [2m/\hbar^2(E - E_0)]^{1/2}$. Dotted line: back-Fourier-transform of the first peak appearing in the $F(R)$ Fourier transform of $\chi(k)$. Dashed line: envelope of the back-Fourier-transform of the first $F(R)$ peak, representing the backscattering amplitude of the first coordination shell. Note that when Co-Si pairs are involved (three top curves) this amplitude decreases monotonously with k , while when Co-Co pairs are involved (bottom curve) a "rounded bell" shape is observed.

main Auger lines of Si $L_{2,3}VV$ (~ 91 eV) and Co $M_{2,3}VV$ (~ 60 eV) are also shown in Fig. 1. For clean Si (top curve) no EXFAS features are observed, while on Si surfaces covered with 2 and 4 Co monolayers (~ 1.8 and 3.6 Å, respectively), well-defined EXFAS features appear. These modulations, marked by arrows in Fig. 1, strengthen in intensity and shift in energy location with increasing coverage. The Co bulk spectrum has been recorded on a thick Co deposited (≥ 100 Å) on top of Si(111) at room temperature. It is well known that upon those conditions the Co layer reflects all bulk electronic properties. Following the usual EXAFS analysis,^{6,21} EXFAS raw data from Fig. 1 have been background subtracted, transformed in wave-vector k space in order to get the analog EXAFS $\chi(k)$ modulations, using the E_0 threshold energy at the Co $M_{2,3}VV$ Auger line for evaluating the electron wave vector

$$k = [2m/\hbar^2(E - E_0)]^{1/2}.$$

Figure 2 shows these modulations (solid lines). We have also included a spectrum obtained on an epitaxial CoSi_2 layer on Si(111). Fourier integration of $\chi(k)$ modulations into the real R space provides ones with the positions of different neighbors $F(R)$ around the Co excited atoms.

Figure 3 shows the Fourier-transform magnitudes $F(R)$ of the $\chi(k)$ modulations. At low-coverage range (2 and 4 monolayers of Co deposited on Si at room temperature) the first main peaks in the $F(R)$ distribution are located at 1.9 ± 0.05 Å. They correspond to the first coordination shell around Co atoms. The same position is found on the CoSi_2 sample. With increasing coverage these peaks shift towards a distance of 2.1 ± 0.05 Å as found on a bulk Co sample.²² Other peaks observed at

~ 3.3 Å also shift with increasing coverage towards 3.6 Å. They are related to the outer coordination shells. These results suggest that at very low coverages, Co and Si atoms interdiffuse at RT and form an interfacial silicide phase with a Co—Si bond length close to that of CoSi_2 , while at higher coverages an almost pure film is found with a Co—Co bond length similar to that of bulk Co.

In order to assess the nature of the atomic species in the first coordination shell around the Co excited atom, a back-Fourier-transform of the first $F(R)$ peak has been performed^{6,21} and the results are shown as dotted lines in Fig. 2. The envelopes of these oscillating functions are shown as dashed lines in Fig. 2. They should represent the backscattering amplitude of the atomic species in the first coordination shell and constitute a "fingerprint" of the nature of the scattering atoms.²¹ On low-coverage Co/Si interfaces and on CoSi_2 this backscattering amplitude follows a monotonous decrease with k , characteristic of Si backscattering atoms around Co excited atoms.²¹ For pure Co films, on the contrary, the backscattering amplitude displays a "rounded bell" shape, characteristic of $3d$ transition metals.²¹ The backscattering-amplitude analysis gives additional stringent proofs which confirm that on low-coverage Co/Si interfaces and bulk Co only Co-Si and Co-Co pairs are involved in the scattering process of the first coordination shell, respectively.

As regards to the physical mechanisms of EXFAS features, we have shown here that they should not be attributed to long-range diffraction processes because no such modulations have been observed on a clean, well-ordered (7×7) Si(111) surface. We believe that they are readily associated with short-range local EXAFS-like

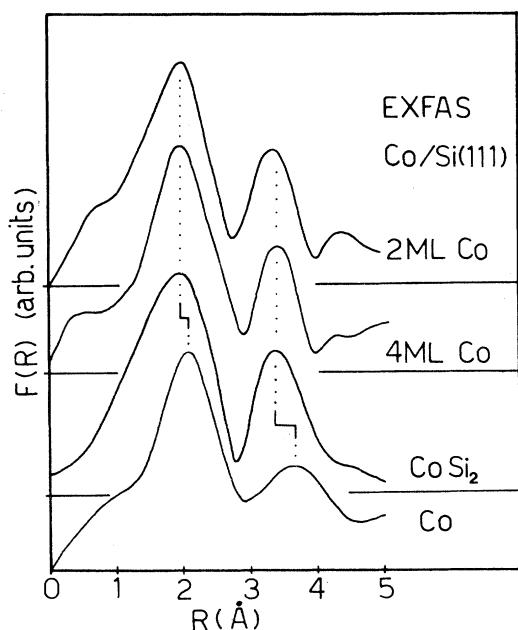


FIG. 3. Fourier-transform magnitude $F(R)$ of the $\chi(k)$ modulations.

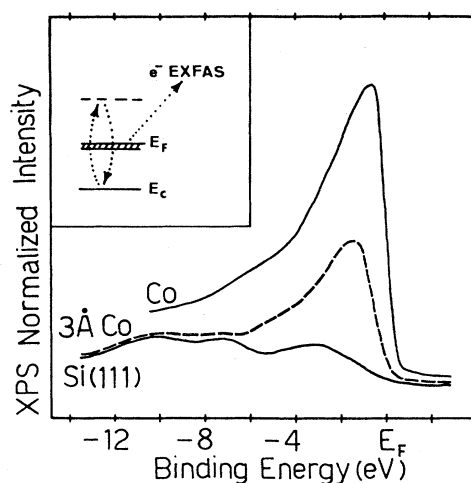


FIG. 4. Valence-band density of states obtained by XPS for clean (bottom curve), 3 Å (middle curve), and ≥ 100 Å (top curve) Co-covered Si surfaces. Spectra are normalized in intensity. Note a narrowing of the valence-band width and an increase in intensity with Co deposition favoring the EXFAS emission. The inset shows schematically the EXFAS principles. An initial core electron at E_c is excited into continuum states above E_f . Its direct recombination with its hole releases an excess energy to excite an electron from the valence band (Ref. 2).

scattering processes since a small amount of Co deposited on Si(111) (and, in general, any narrow, high-density-of-states d metal) provokes the appearance of EXFAS features which take their origin from emission of valence electrons. Figure 4 shows the valence-band density of states (DOS) as measured by x-ray-induced photoelectron spectroscopy for clean and Co-covered Si surfaces. The three spectra are normalized in intensity in order to get a significant comparison. The low Si DOS extends on about 12–16-eV energy range, while the high DOS of the Co-Si interface is mainly concentrated in ~ 4 –5 eV. During the autoionization process which gives rise to the EXFAS emission, described schematically in the inset, Fig. 4, the EXFAS yield depends strongly on the valence-band DOS intensity. The larger valence-band width is, the weaker the EXFAS modulations. This is the reason why no EXFAS features are observed on a well-ordered (7×7) Si(111) surface displaying a low DOS and large valence-band width while on disordered Co/Si(111) (no LEED pattern) with a high DOS and narrow valence-band width, well-defined EXFAS features are

detected, favoring the short-range local EXAFS-like scattering explanation. This conclusion is also reached by one of us²³ looking at the influence of thermal disorder on the Cu/Ag (111) system with the EXFAS technique. These authors observe an EXAFS-like behavior with a progressive disappearance of the *outer* shells with increasing temperature in contrast with LEED behavior where all diffraction spots should disappear together.

In summary, thanks to a detailed comparison of the influence of static disorder on the Co/Si interface at room temperature we aim to explain conclusively the physical origins of the EXFAS mechanisms. The EXFAS results presented here (i) agree with other studies on the Co/Si interface, (ii) confirm our previous calculations which predict that such EXAFS-like modulations should be observed in energy range above Auger lines,² and (iii) open the way to investigate the short-range local order (bond length and coordination nature) of most metal-semiconductor interfaces (and, in general, most surface and interface studies).

*Permanent address: Dipartimento di Fisica, Seconda Università degli Studi di Roma, Tor Vergata, via Orazio Raimondo, I-00173 Roma, Italy.

¹See a review paper by R. Weissmann and K. Müller, *Surf. Sci. Rep.* **1**, 251 (1981).

²J. Derrien, E. Chainet, M. De Crescenzi, and C. Noguerra, *Surf. Sci.* **189/190**, 590 (1987); M. De Crescenzi, E. Chainet, and J. Derrien, *Solid State Commun.* **57**, 487 (1986).

³E. A. Stern, D. E. Sayers, and F. W. Lytle, *Phys. Rev. B* **11**, 4836 (1975).

⁴G. Zajac, J. Zak, and S. D. Bader, *Phys. Rev. Lett.* **50**, 1713 (1983); *Phys. Rev. B* **29**, 5491 (1984); C. J. Powell and N. E. Erickson, *Phys. Rev. Lett.* **51**, 61 (1983); Y. Sakisaka, T. Miyano, and M. Onchi, *ibid.* **54**, 714 (1985).

⁵J. E. Müller and J. W. Wilkins, *Phys. Rev. B* **29**, 4331 (1984).

⁶See, for example, P. A. Lee, P. M. Citrin, P. Eisenberger, and B. M. Kincaid, *Rev. Mod. Phys.* **53**, 769 (1981).

⁷L. McDonnell, B. D. Powell, and D. P. Woodruff, *Surf. Sci.* **40**, 669 (1973).

⁸G. E. Becker and H. D. Hagstrum, *J. Vac. Sci. Technol.* **11**, 284 (1974).

⁹See a review paper by J. Derrien, *Surf. Sci.* **168**, 171 (1986).

¹⁰S. Saitoh, H. Ishima, and S. Furukawa, *Appl. Phys. Lett.* **37**, 203 (1980).

¹¹R. T. Tung, J. M. Gibson, and J. M. Poate, *Phys. Rev. Lett.* **50**, 429 (1983).

¹²L. J. Chen, J. W. Mayer, and K. N. Tu, *Thin Solid Films* **93**, 135 (1982).

¹³C. Pirri, J. C. Peruchetti, G. Gewinner, and J. Derrien, *Phys. Rev. B* **29**, 3391 (1984).

¹⁴F. Boscherini, J. J. Joyce, M. W. Ruckman, and J. H. Weaver, *Phys. Rev. B* **35**, 4216 (1987).

¹⁵See a review paper by J. Derrien and F. Arnaud d'Avitaya, *J. Vac. Sci. Technol.* **5**, 2111 (1987); C. d'Anterrosches, *Surf. Sci.* **168**, 751 (1986).

¹⁶E. Rosencher, S. Delage, Y. Campidelli, and F. Arnaud d'Avitaya, *Electron. Lett.* **20**, 762 (1984).

¹⁷J. C. Hensel, R. T. Tung, J. M. Poate, and F. C. Unterwald, *Appl. Phys. Lett.* **47**, 151 (1984).

¹⁸E. Chainet, M. De Crescenzi, J. Derrien, T. T. A. Nguyen, and R. C. Cinti, *Surf. Sci.* **168**, 309 (1986).

¹⁹J. Y. Veuillen, J. Derrien, P. A. Badoz, E. Rosencher, and C. d'Anterrosches, *Appl. Phys. Lett.* **51**, 1448 (1987).

²⁰J. Derrien, M. De Crescenzi, E. Chainet, and C. d'Anterrosches, *Phys. Rev. B* **36**, 6681 (1987).

²¹B. K. Teo, *EXAFS: Basic principles and data analysis. Inorganic Chemistry Concepts* (Springer-Verlag, Berlin, 1986), Vol. 9; B. K. Teo and P. A. Lee, *J. Am. Chem. Soc.* **101**, 2815 (1979).

²²In order to derive the true crystallographic value R , one needs to add to the experimental value a ΔR due to the phase shift according to EXAFS principles. For $M_{2,3}$ edges ΔR amounts to ~ 0.45 Å. See, for example, E. Chainet, M. De Crescenzi, and J. Derrien, *Phys. Rev. B* **31**, 7469 (1985).

²³T. Tyliczszak, A. P. Hitchcock, and M. De Crescenzi, *Phys. Rev. B* **38**, 5768 (1988).